



CHORUS

This is the accepted manuscript made available via CHORUS. The article has been published as:

Model analysis of magnetic susceptibility of $\text{Sr}_{\{2\}}\text{IrO}_{\{4\}}$: A two-dimensional $J_{\text{eff}}=1/2$ Heisenberg system with competing interlayer couplings

Tomohiro Takayama, Akiyo Matsumoto, George Jackeli, and Hidenori Takagi

Phys. Rev. B **94**, 224420 — Published 20 December 2016

DOI: [10.1103/PhysRevB.94.224420](https://doi.org/10.1103/PhysRevB.94.224420)

Model analysis of magnetic susceptibility of Sr_2IrO_4 - 2D $J_{\text{eff}} = 1/2$ Heisenberg system with competing interlayer couplings

Tomohiro Takayama,^{1,2} Akiyo Matsumoto,² George Jackeli,^{1,3} and Hidenori Takagi^{1,2,3}

¹*Max Planck Institute for Solid State Research, Heisenbergstrasse 1, 70569 Stuttgart, Germany*

²*Department of Physics and Department of Advanced Materials, University of Tokyo, 7-3-1 Hongo, Tokyo 113-0033, Japan*

³*Institute for Functional Matter and Quantum Technologies, University of Stuttgart, Pfaffenwaldring 57, 70569 Stuttgart, Germany*

(Dated: November 30, 2016)

We report the analysis of magnetic susceptibility $\chi(T)$ of Sr_2IrO_4 single crystal in the paramagnetic phase. We formulate the theoretical susceptibility based on isotropic Heisenberg antiferromagnetism incorporating the Dzyaloshinsky-Moriya interaction exactly, and include the interlayer couplings in a mean-field approximation. $\chi(T)$ above T_N was found to be well described by the model, indicating the predominant Heisenberg exchange consistent with the microscopic theory. The analysis points to a competition of nearest and next-nearest neighbor interlayer couplings, which results in the up-up-down-down configuration of the in-plane canting moments identified by the diffraction experiments.

PACS numbers: 75.30.-m, 75.30.Cr, 75.30.Et

I. INTRODUCTION

Complex iridium oxides recently emerged as a novel playground for correlated electron physics where strong spin-orbit coupling of $5d$ Ir, comparable to its modest Coulomb U , plays a critical role to produce unprecedented electronic phases. A notable example is the spin-orbital Mott state with local $J_{\text{eff}} = 1/2$ wave function produced by the interplay between spin-orbit coupling and Coulomb U . The $J_{\text{eff}} = 1/2$ wave function consists of equally weighted superposition of three t_{2g} orbitals with imaginary components, $|J_{\text{eff}} = \pm 1/2 \rangle = \frac{1}{\sqrt{3}}\{|d_{xy}, \pm\sigma \rangle \pm |d_{yz}, \mp\sigma \rangle + i|d_{zx}, \mp\sigma \rangle\}$ where σ denotes the spin state [1]. The $J_{\text{eff}} = 1/2$ Mott state was first identified in the K_2NiF_4 -type layered perovskite Sr_2IrO_4 [2]. In spin-orbital Mott insulators, the magnetic coupling between $J_{\text{eff}} = 1/2$ pseudo-spins is mediated by their direct overlap or superexchange interaction via anions, and is therefore critically affected by the unique form of $J_{\text{eff}} = 1/2$ wave function.

The magnetic coupling between $J_{\text{eff}} = 1/2$ pseudo-spins was studied theoretically in Ref. [3], and the low energy Hamiltonian was constructed. In the case of 90° bond of Ir-O-Ir, where the IrO_6 octahedra share their edges, the destructive interference manifests itself in the two superexchange paths of Ir-O₂-Ir plaquette owing to the imaginary components of $J_{\text{eff}} = 1/2$ state. As a consequence, the magnetic exchange takes the form of an anisotropic bond-dependent interaction. Such bond-dependent coupling gives rise to strong frustration when iridium ions are placed on a tri-coordinated motif like honeycomb lattice, invoking a possible route for Kitaev spin liquid [4]. In contrast, for 180° bond of Ir-O-Ir, relevant to Sr_2IrO_4 , the magnetic coupling is proposed to comprise isotropic Heisenberg exchange and pseudodipolar interaction stemming from Hund's coupling. The

emergence of isotropic Heisenberg coupling, rooted in the isotropic $J_{\text{eff}} = 1/2$ wave function, is rather unexpected since spin-orbit coupling is generally considered to produce magnetic anisotropy.

The presence of Heisenberg coupling was indeed found experimentally in Sr_2IrO_4 . Sr_2IrO_4 undergoes a magnetic transition around $T_N \sim 240$ K [5]. A resonant x-ray diffuse scattering showed that the two-dimensional (2D) magnetic correlation survives in the IrO_2 planes above T_N [6], and the temperature dependence of correlation length obeys the relation theoretically proposed for the 2D $S = 1/2$ isotropic Heisenberg antiferromagnetism (IHAF) on a square lattice [7]. The nearly gapless magnon dispersion observed by resonant inelastic x-ray scattering (RIXS) is consistent with those expected for IHAF [8]. The 2D IHAF of Sr_2IrO_4 is reminiscent of the isostructural compound La_2CuO_4 , a parent Mott insulator of high- T_c superconductor with 2D $S = 1/2$ IHAF [9, 10]. The similarity of two compounds led the theoretical prediction of possible superconductivity in Sr_2IrO_4 upon doping [11–13] and the observation of Fermi arcs and d -wave gap on the doped surface of Sr_2IrO_4 [14–16].

Despite the strong 2D character of Heisenberg exchange, Sr_2IrO_4 orders antiferromagnetically likely due to a small but finite interlayer coupling, which is also the case of La_2CuO_4 . The magnetic structure of Sr_2IrO_4 was revealed by resonant x-ray magnetic scattering [2] as illustrated in Fig. 1. Below T_N , the $J_{\text{eff}} = 1/2$ pseudo-spins lying in the basal planes form a Néel order. Since the crystal structure of Sr_2IrO_4 has the staggered rotations of IrO_6 octahedra about the c -axis ($\sim 11^\circ$) [17], Dzyaloshinsky-Moriya (DM) interaction with \mathbf{D} parallel to the c -axis is present [3], leading to canting of pseudo-spins and the appearance of small in-plane moment. The in-plane canting moments are cancelled out at zero field by forming the up-up-down-down (uudd) stacking configuration along the c -axis [Fig. 1(a)], while at a field above

$\mu_0 H_c \sim 0.2$ T the in-plane moments align and produce weak-ferromagnetism with a moment M of $\sim 0.075\mu_B/\text{Ir}$ [2]. This magnetic structure of Sr_2IrO_4 resembles with that of La_2CuO_4 . In La_2CuO_4 , $S = 1/2$ spins order antiferromagnetically, and the buckling distortion of CuO_6 produces in-plane canting moments normal to the CuO_2 planes through DM interaction, which stack antiferromagnetically along the c -axis.

The uudd configuration of canting moments in Sr_2IrO_4 at a glance would suggest the presence of two different interlayer couplings between the neighboring IrO_2 planes. Considering the crystal structure, however, the interlayer couplings between the adjacent planes are all equivalent. In order to account for the uudd configuration, the interlayer couplings beyond the nearest neighbors must be taken into account.

Thio et al. formulated the magnetic susceptibility $\chi(T)$ of La_2CuO_4 by a mean-field approximation with the DM interaction and the interlayer coupling [18, 19], which well reproduced the experimental data, and confirmed the predominant 2D Heisenberg exchange in the CuO_2 planes. Sr_2IrO_4 inherits stronger DM interaction due to spin-orbit coupling of Ir, as evidenced by the much larger canting moment compared with that of La_2CuO_4 ($M \sim 2 \times 10^{-3}\mu_B/\text{Cu}$) [18]. **Unlike La_2CuO_4 , the strength of DM interaction in Sr_2IrO_4 is solely determined by lattice distortions, the staggered rotations of octahedra [3].** As a critical test for the 2D IHAF, similar mean-field analysis on Sr_2IrO_4 is desired.

In this paper, we present the analysis of $\chi(T)$ of Sr_2IrO_4 in the paramagnetic phase above T_N . We formulated the theoretical magnetic susceptibility based on the Heisenberg model incorporating DM interaction and introduced the interlayer couplings within a mean-field approximation. The experimental data were fitted by the theoretical susceptibility, and the analysis indicates that $\chi(T)$ is fully consistent with the predominance of isotropic Heisenberg exchange. The parameters obtained by the fit point to a competing nature of nearest and next-nearest interlayer couplings.

II. EXPERIMENTAL

Single crystals of Sr_2IrO_4 were grown by using SrCl_2 flux [2]. Magnetization data were collected by a commercial magnetometer (Quantum Design, MPMS). In order to obtain sizable magnetization signal at low fields, ~ 20 thin plate-like single crystals (~ 2 mm \times 2 mm \times 0.05 mm) were piled up to form a block-shaped sample (~ 18 mg). The background contribution from the sample holder was measured independently, and was subtracted from the raw magnetization data.

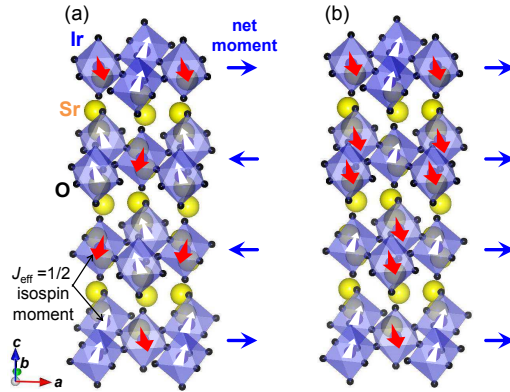


FIG. 1. Crystal and magnetic structures of Sr_2IrO_4 (a) at zero magnetic field, and (b) above metamagnetic critical field $\mu_0 H_c \sim 0.15$ T. Yellow, blue and black spheres represent Sr, Ir and O atoms, respectively [41]. Red and white arrows on Ir atoms depict the directions of $J_{\text{eff}} = 1/2$ isospin moments, and blue arrows show the directions of net in-plane canting moments.

III. RESULTS

The temperature dependent magnetic susceptibility, measured at a low field of 0.1 T, is shown in Fig. 2. A large anisotropy between the in-plane ($\chi_{ab} \equiv M_{ab}/H$) and the out-of-plane ($\chi_c \equiv M_c/H$) susceptibilities is clearly seen [20]. Only χ_{ab} displays a pronounced temperature dependence roughly below room temperature, while χ_c remains almost constant over the whole temperature range measured. The observed anisotropy should be attributed to the in-plane canting moments produced by DM interaction with $\mathbf{D} \parallel$ the c -axis.

In the in-plane susceptibility χ_{ab} , a peak is observed around 200 K which is lower than $T_N \sim 230$ K determined by a magnetic x-ray diffraction measurement [6]. T_N appears to be reflected as the peak temperature in the temperature derivative of susceptibility, namely the temperature with the steepest slope in rapidly increasing susceptibility on cooling to the peak at 200 K (see the lower inset of Fig. 2). In contrast to the previous data measured at a relatively high field of 0.5 T [5], χ_{ab} shows a clear decrease with cooling below 200 K. This is consistent with the uudd stacking of canting moments in the ground state [2], where the net moments are zero. The bifurcation **between the zero-field cooling (ZFC) and field-cooling (FC) data**, seen well below T_N , likely represents the uncompensated canting moments due to the pinning to crystalline defects such as stacking faults along the c -axis. We believe that the competition of very weak nearest and next-nearest interlayer couplings, as will be discussed below, is one of the origins for such pronounced pinning effect.

In the isothermal magnetization curve at 5 K well below T_N , shown in Fig. 3, a metamagnetic transition from

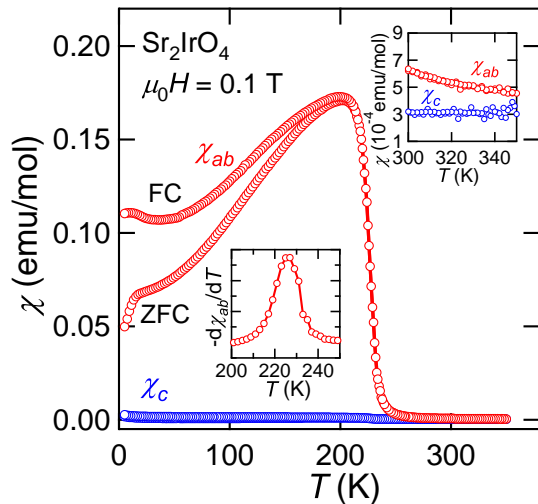


FIG. 2. Temperature dependence of in-plane (χ_{ab}) and out-of-plane (χ_c) magnetic susceptibilities of Sr_2IrO_4 measured at 0.1 T. ZFC and FC denote the zero-field-cooling and field-cooling curves for χ_{ab} , respectively. The lower inset shows the temperature derivative of in-plane susceptibility which shows a peak at ~ 230 K, and the upper one displays the magnified view of high-temperature region.

an antiferromagnetic ground state to a weak ferromagnetic state can be seen [5]. A sudden increase of the in-plane magnetization at around $\mu_0 H_c \sim 0.15$ T was observed, which corresponds to the flipping of net in-plane moments as illustrated in Fig. 1. The reduced slope at the zero field limit mirrors the suppressed in-plane susceptibility below 200 K in the temperature dependent susceptibility. Measuring the magnetization above $\mu_0 H_c$ gives rise to a weakly ferromagnetic behavior as reported previously [5]. The magnitude of weak ferromagnetic moments is $\sim 0.068 \mu_B/\text{Ir}$, slightly smaller than a reported value of $\sim 0.075 \mu_B/\text{Ir}$ [2]. (100) orientation of moment (in the $\sqrt{2}a \times \sqrt{2}a$ unit cell where a is the nearest Ir-Ir distance) is known to be realized in the ordered state under zero field [21]. However, any appreciable anisotropy in the magnetization curve was not detected between the (100) and (110) directions as shown in Fig. 3. The in-plane anisotropy should be finite but extremely small. We do not observe any trace of metamagnetism along the c -axis, consistent with the canting moments only within the ab -planes by $\mathbf{D} //$ the c -axis [22]. Since the metamagnetism is associated with a change in the magnetic interlayer sequence along the c -axis, we can estimate the effective interlayer coupling energy as the product of the metamagnetic moment ΔM_{ab} and the critical magnetic field H_c as $\Delta M_{ab} \cdot \mu_0 H_c \sim 0.06 \mu_B \times 0.15 \text{ T} \sim 0.7 \mu\text{eV}$. There is a hysteresis in the magnetization at a low field region, which shows up as the bifurcation in the temperature dependent susceptibility and should be extrinsic.

With increasing temperature above T_N , χ_{ab} decreases

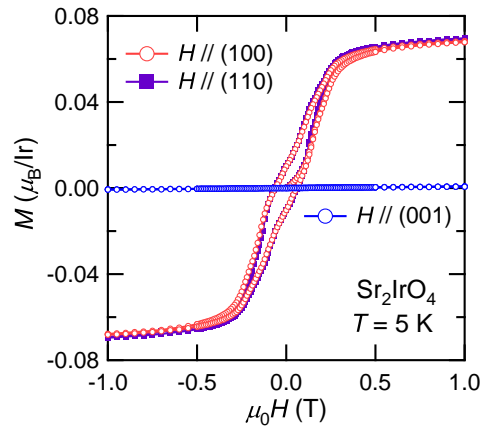


FIG. 3. Isothermal magnetization curves of Sr_2IrO_4 registered at 5 K.

and appears to crossover to almost temperature independent behavior. The magnitude of χ_{ab} in the high temperature limit is comparable to χ_c as seen in the upper inset of Fig. 2, implying that the isospin system is isotropic in the paramagnetic phase. We will analyze this region in detail as a weakly coupled 2D Heisenberg system with DM interaction.

IV. DISCUSSION

A. Fitting of $\chi(T)$ based on 2D IHAF model.

The interlayer coupling energy is orders of magnitude smaller than that of the in-plane coupling characterized by the in-plane antiferromagnetic coupling $J_{ab} \sim 0.1$ eV [6, 23]. This should give rise to strong 2D magnetic fluctuations over a wide temperature range up to $\sim J_{ab}/k_B$ well above the three-dimensional ordering temperature T_N . The Heisenberg character of 2D fluctuations was captured as the temperature dependence of magnetic correlation length above T_N measured by a resonant x-ray diffuse scattering [6]. As described in the introduction, the magnetism of $J_{\text{eff}} = 1/2$ pseudo-spins is in striking parallel with the case for 2D $S = 1/2$ Heisenberg antiferromagnet La_2CuO_4 . The two-dimensional magnetic correlations ($J_{ab} \sim 0.135$ eV [19]) first develop on cooling, and the finite interlayer coupling ($\sim 1 \mu\text{eV}$) triggers the three-dimensional magnetic ordering at T_N [10, 18].

In accord with the close analogy of $J_{\text{eff}} = 1/2$ magnetism of Sr_2IrO_4 with 2D $S = 1/2$ IHAF in La_2CuO_4 , we emphasize here that the temperature dependent magnetic susceptibility $\chi(T)$ of La_2CuO_4 is surprisingly similar to that of Sr_2IrO_4 . The out-of-plane susceptibility χ_c of La_2CuO_4 displays a sharp peak at T_N while the in-plane susceptibility $\chi_{ab}(T)$ shows only a very weak temperature dependence [18, 24]. A clear signature of metamagnetism was observed below T_N in the out-of-plane

magnetization curve, evidencing the presence of canting moments [18, 19, 24].

In La_2CuO_4 , the steep increase of $\chi_c(T)$ right above T_N is attributed to the canting moment produced by DM interaction in the presence of developed 2D magnetic correlations. The theoretical magnetic susceptibility formulated by Thio et al., which is based on 2D IHAF incorporating DM interaction and interlayer coupling, well described $\chi(T)$ of La_2CuO_4 [18, 19]. In the following, we attempt to describe $\chi(T)$ of Sr_2IrO_4 in the same framework.

In order to formulate $\chi(T)$ of Sr_2IrO_4 , two major differences from La_2CuO_4 must be taken into account. (i) In Sr_2IrO_4 , the rotation of IrO_6 octahedra about the c -axis gives rise to the DM vector parallel to the c -axis, whereas the buckling of CuO_6 along (010) (in the $\sqrt{2}a \times \sqrt{2}a$ unit cell) yields the DM vector lying in the CuO_2 plane. This results in the direction of the canting moments parallel to the IrO_2 plane in Sr_2IrO_4 , while that is perpendicular to the CuO_2 plane in La_2CuO_4 . (ii) The interlayer coupling is dominated by nearest neighbor antiferromagnetic interaction in La_2CuO_4 . For Sr_2IrO_4 , the interlayer couplings beyond the nearest neighboring planes must be considered to allow for the uudd configuration of canting moments. With these differences in mind, we construct the theoretical magnetic susceptibility of Sr_2IrO_4 in the paramagnetic phase.

To derive the theoretical magnetic susceptibility, we introduce the local axes for A and B magnetic sublattices. They are obtained by a staggered rotation of spin-axis about z -axis (i.e. the crystallographic c -axis) with angles of $\pm\phi$, as sketched in the inset of Fig. 4. In the rotated axis frame, the intralayer magnetic coupling can be mapped onto IHAF, if we ignore the Hund's coupling, as discussed in Ref. [3]. By introducing the interlayer couplings in a mean-field approximation, the in-plane susceptibility of 3D coupled layers is expressed as follows in terms of its out-of-plane component χ_c and staggered susceptibility of 2D IHAF χ^\dagger given in units of inverse energy. We find (see Appendix),

$$\chi_{ab} = \cos^2 \phi \chi_c + \frac{\sin^2 \phi (g_{ab} \mu_B)^2 \chi^\dagger}{1 - J_c \chi^\dagger} \quad (4.1)$$

where μ_B and g_{ab} denote respectively Bohr magneton and the in-plane g -factor of $J_{\text{eff}} = 1/2$ isospin, which is 2 in the cubic limit [1]. For the interlayer couplings, we first consider a single parameter J_c which represents an effective exchange field coming from all interlayer exchange couplings.

We analyze the experimental in-plane susceptibility in the paramagnetic phase shown in Fig. 4 based on Eq. (4.1). The out-of-plane susceptibility χ_c is independent of temperature in the range shown in Fig. 4, and estimated to be 3.1×10^{-4} emu/mol [25]. Makivic and Ding studied the $S = 1/2$ 2D Heisenberg model on a square lattice by quantum Monte Carlo simulation, and obtained the following relation for staggered susceptibility χ^\dagger ,

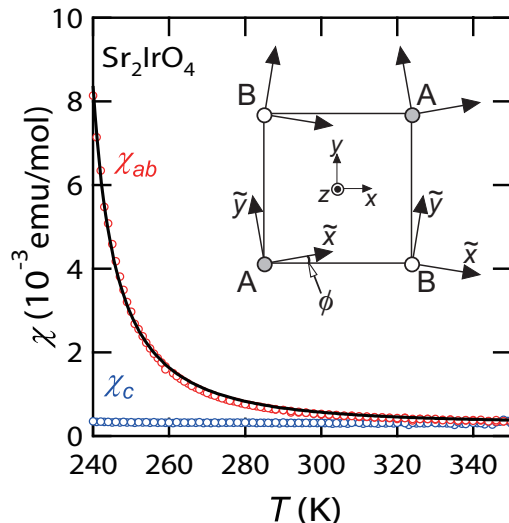


FIG. 4. Magnetic susceptibilities of Sr_2IrO_4 in the high-temperature paramagnetic phase. Red and blue dots show the experimental in-plane (χ_{ab}) and out-of-plane (χ_c) susceptibilities, and the black solid line delineates the fitting line for χ_{ab} based on Eq. (4). The inset depicts the local spin frame (\tilde{x} , \tilde{y}) rotated by the angle of $\pm\phi$ from the laboratory frame of (x , y). A and B represent the two antiferromagnetic sublattices.

$$\chi^\dagger = 1.65(\xi/a)^2 (k_B T / J_{ab}^2) \quad (4.2)$$

where ξ is the two-dimensional magnetic correlation length and a is the nearest Ir-Ir distance [26]. ξ is expressed as,

$$\xi = 0.276 a \exp(1.25 J_{ab} / T) \quad (4.3)$$

which well explained the experimental data obtained by resonant x-ray diffuse scattering and yielded J_{ab} as 0.1 ± 0.01 eV [6]. We note that χ^\dagger estimated from Eq. (4.2) agrees well with the one obtained by a large scale quantum Monte Carlo method [27].

Throughout the analysis, we employed the following assumptions so as to obtain a reliable fit. (i) Since ϕ is at most $\sim 11^\circ$, which is the angle of IrO_6 rotations about the c -axis, $\cos^2 \phi$ should be $0.97 < \cos^2 \phi < 1$, namely very close to 1. We thus omitted the prefactor of $\cos^2 \phi$ for the out-of-plane susceptibility χ_c . We confirmed that the presence or absence of this factor did not alter the final results [28]. (ii) Since g_{ab} and ϕ cannot be determined independently, we treated $g_{ab} \sin \phi$ as a single parameter. By taking J_c and $g_{ab} \sin \phi$ as variant parameters and fixing J_{ab} at 0.10 eV, we fitted the experimental in-plane susceptibility in the temperature range between 240 K and 350 K [28].

The result of fit is shown as the black solid line in Fig. 4. Eq. (4.1) reasonably reproduces the experimental result, indicating the predominance of IHAF in

Sr_2IrO_4 . This also implies that the influence of pseudodipolar interaction induced by Hund's coupling is not appreciable in the high temperature paramagnetic phase of Sr_2IrO_4 [29]. **The observed strong temperature dependent upturn of in-plane susceptibility is solely due to anisotropic DM interaction induced linear coupling of uniform and staggered (critical) components of χ_{ab} , while Hund's coupling induced easy-plane anisotropy, not considered here, would merely induce small constant shift of χ_{ab} within the temperature range discussed here.** The obtained parameters are $g_{ab}\sin\phi = 0.0376 \pm 0.0002$ and $J_c = 15.86 \pm 0.07 \mu\text{eV}$. We note that a steep increase of χ_{ab} right above T_N by DM interaction benefits in obtaining a reliable fit. This contrasts with a sister compound Ba_2IrO_4 where DM interaction is absent and its magnetic susceptibility shows no visible anomaly at T_N [30].

The obtained $g_{ab}\sin\phi \sim 0.038$ is small compared with the one estimated from the weak ferromagnetic moment in the ordered state at low temperatures, $M = g_{ab}\mu_B S\sin\phi \sim 0.068 \mu_B$. For $S = 1/2$, the $g_{ab}\sin\phi \sim 0.13$, a factor of 3 larger than the fitting result. **The isospin moments of Sr_2IrO_4 are known to rigidly follow the IrO_6 rotations [31] by DM interaction with strong spin-orbit coupling.** Since the change of IrO_6 rotation angle is less than 1° between room temperature and 10 K [32], we cannot ascribe the difference to the change of isospin canting angle by temperature. The possible origin of this discrepancy is the reduced magnitude of isospin moments at high temperatures. Due to the smallness of charge gap of ~ 0.5 eV [1], charge excitation is substantial at high temperatures which may renormalize the size of effective local moment. Such renormalization might be a characteristic feature of weak Mott insulators with a small charge gap.

B. Up-up-down-down stacking configuration of in-plane canting moments.

The fitting result shows an effective antiferromagnetic interlayer coupling $J_c > 0$. If only the nearest plane interlayer coupling is considered, this cannot lead to the uudd interlayer sequence of in-plane moments, and the interlayer couplings beyond nearest planes must be taken into account. The presence of sizable further neighbor interlayer couplings should be reasonable in the sense that Sr_2IrO_4 is regarded as a weak Mott insulator marginally formed by modest Coulomb U of $5d$ electrons. Since the interlayer couplings beyond the next-nearest neighboring planes are supposed to be negligibly small, we consider the interlayer couplings from the nearest and next-nearest planes.

We construct a minimal model that includes the isotropic couplings between iridium ions in nearest (J'_{1c} and J''_{1c}) within the same and different sublattices, respectively) and next-nearest (J_{2c}) planes (see Fig. 5). **It takes the following form:**

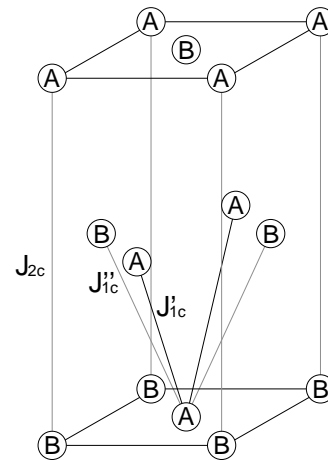


FIG. 5. Interlayer couplings in nearest (J'_{1c} and J''_{1c}) and next-nearest (J_{2c}) planes. The iridium sublattice formed by anticlockwise (clockwise) rotated octahedra is labeled by A (B).

$$\begin{aligned} \mathcal{H}_c = & \sum_n J'_{1c} (\vec{S}_{A,n} \cdot \vec{S}_{A,n+1} + \vec{S}_{B,n} \cdot \vec{S}_{B,n+1}) \quad (4.4) \\ & + \sum_n J''_{1c} (\vec{S}_{A,n} \cdot \vec{S}_{B,n+1} + \vec{S}_{B,n} \cdot \vec{S}_{A,n+1}) \\ & + \sum_n J_{2c} (\vec{S}_{A,n} \cdot \vec{S}_{B,n+2} + \vec{S}_{B,n} \cdot \vec{S}_{A,n+2}), \end{aligned}$$

where $\vec{S}_{A(B),n}$ denotes spins of A(B) sublattice of n th-layer in the laboratory frame. The fact that there is no visible anisotropy in the measured in-plane magnetizations justifies to drop out symmetry allowed anisotropy terms. By introducing the planar unit vector \vec{m}_n for the staggered moment of n th-layer, which corresponds to $(\vec{S}_{A,n} - \vec{S}_{B,n})/2S$ where $\vec{S}_{A(B),n}$ denotes spins in the local (rotated) frame, we arrive to the following classical energy (in unit of $1/S^2$) of coupled layers,

$$E = \sum_n \{ -j_{1c} \vec{m}_n \cdot \vec{m}_{n+1} + j_{2c} \vec{m}_n \cdot \vec{m}_{n+2} - b(\vec{m}_n \cdot \vec{m}_{n+1})^2 \}, \quad (4.5)$$

where $j_{1c} = 2(J''_{1c} \cos 2\phi - J'_{1c})$ and $j_{2c} = -J_{2c} \cos 2\phi$ are effective exchange couplings between nearest and next-nearest neighbor planes, respectively [33, 34]. In addition to the classical energy, we also include effective bi-quadratic coupling b driven by quantum fluctuations [35]. In order to allow for the uudd configuration, we assume ferromagnetic (antiferromagnetic) nearest (next-nearest) interlayer couplings between \vec{m}_n , respectively [34].

The effective interlayer coupling J_c , entering in Eq. (4.1), is expressed as $J_c = 2(j_{1c} - j_{2c})$. From the fit value of $J_c \sim 15.9 \mu\text{eV}$ and the change of exchange energy at the field induced metamagnetic transition $(2j_{1c} - j_{2c})S^2 = \Delta M_{ab} \cdot \mu_0 H_c \sim 0.7 \mu\text{eV}$, we obtain

j_{1c} and j_{2c} as $18.8 \mu\text{eV}$ and $10.8 \mu\text{eV}$, respectively. The result points to a competition of nearest and next-nearest interlayer couplings with a comparable magnitude, which originates from the following facts; (i) j_{1c} is geometrically frustrated, that is, J'_{1c} and J''_{1c} compete each other and j_{1c} is marginally yielded by the uncompensated out-of-plane exchanges due to the rotational distortion of IrO_6 octahedra. (ii) The cubic character of $J_{\text{eff}} = 1/2$ wave function, in contrast to the outermost Cu $d_{x^2-y^2}$ orbital of La_2CuO_4 extended in the basal plane, gives rise to sizable J_{2c} .

The result accounts for the uudd configuration of in-plane moments observed by the diffraction experiments [2, 21]. The uudd configuration is stabilized in the following parameter range of the present model [Eq. (4.5)] [36],

$$2j_{2c} > j_{1c} > 0 \text{ and } b > \frac{j_{1c}^2}{4(2j_{2c} - b)} > 0. \quad (4.6)$$

j_{1c} and j_{2c} obtained as above satisfy the former relation. The latter relation calls for $b > 5.5 \mu\text{eV}$, which is three orders of magnitude larger than the value reported for La_2CuO_4 ($b \sim 2 \times 10^{-9} \text{ eV}$) [35]. Since b is in proportion to $J_{\text{out}}^2 S/J_{ab}$, where J_{out} is the isotropic exchange between nearest neighbors in the adjacent planes ($J_{\text{out}} \sim J'_{1c}$ or J''_{1c}), this suggests the larger interlayer coupling J_{out} and thus larger interlayer hopping t_{\perp} in Sr_2IrO_4 . In a crude estimation [37], we obtain $t_{\perp}(\text{Sr}_2\text{IrO}_4) \sim 5 t_{\perp}(\text{La}_2\text{CuO}_4)$. The larger t_{\perp} of Sr_2IrO_4 is consistent with the smaller anisotropy of resistivity ρ_c/ρ_a of Sr_2IrO_4 than that of La_2CuO_4 [11], again attributed to the weak Mott character and the cubic shape of $J_{\text{eff}} = 1/2$ wave function. The uudd configuration of in-plane moments in Sr_2IrO_4 is therefore stabilized by the following factors; (i) geometrically frustrated nature of nearest neighbour interlayer couplings which suppresses j_{1c} , (ii) isotropic and extended character of $J_{\text{eff}} = 1/2$ wave function giving rise to sizable j_{2c} and b .

V. CONCLUSION

We analyzed the magnetic susceptibility of spin-orbital Mott insulator Sr_2IrO_4 in the paramagnetic phase. The analysis evidences the predominance of isotropic Heisenberg exchange between the $J_{\text{eff}} = 1/2$ pseudo-spins, further reinforcing the similarity with La_2CuO_4 . The result of fit points to the competing interlayer couplings between the nearest and next-nearest IrO_2 planes. The competing nature of interlayer couplings and the resultant complex stacking pattern of $J_{\text{eff}} = 1/2$ isospin moments might give a clue for further unsettled issues of Sr_2IrO_4 such as high-pressure suppression of weak-ferromagnetic moments [38] and the second magnetic transition below T_N argued from the local probes [39].

ACKNOWLEDGEMENTS

We are grateful to G. Khaliullin, V. Kataev, P. Lemmens and B. Keimer for invaluable discussion and R. Kremer for technical support. This work is partly supported by Grant-in-Aid for Scientific Research (S) (Grant No. 24224010) and Grant-in-Aid for Scientific Research on Innovative Areas (Grant No. JP15H05852) from JSPS of Japan. G.J. is supported in part by the National Science Foundation under Grant No. NSF PHY11-25915.

APPENDIX

In this Appendix, we derive the in-plane susceptibility of 3D coupled layer system in terms of uniform and staggered susceptibilities of 2D IHAF. The exchange interactions for an intralayer bond of nearest-neighbor iridium ions can be written as:

$$\mathcal{H}_{ij} = J\vec{S}_i \cdot \vec{S}_j + J_z S_i^z S_j^z - D(S_i^x S_j^y - S_i^y S_j^x), \quad (\text{A1})$$

they include isotropic antiferromagnetic (AF) coupling (J), as well as symmetric (J_z) and antisymmetric (D) Dzyaloshinsky-Moriya (DM) exchange anisotropies [3]. The dominant contributions (ignoring Hund's exchange induced corrections) to the coupling constants in Eq. A1 can be parameterized as $J = J_{ab} \cos 2\phi$, $J_z = 2J_{ab} \sin^2 \phi$, and $D = J_{ab} \sin 2\phi$, where $J_{ab} = \sqrt{J^2 + D^2}$ defines overall energy scale of intralayer exchange and $\tan 2\phi = D/J$. Following Ref. [3], we introduce the local quantization axes for spins on A and B sublattices obtained by a staggered rotation of the spin frame around z -axis by an angle $\pm\phi$ [see inset in Fig. 4 of the main text]. We further denote by \tilde{S}_i^γ ($\gamma = x, y, z$) the Cartesian components of spins in a local rotated frame. They are related to the laboratory frame by the following transformations:

$$\begin{aligned} S_i^x &= \cos \phi \tilde{S}_i^x - \exp(i\mathbf{Q}\mathbf{R}_i) \sin \phi \tilde{S}_i^y, \\ S_i^y &= \cos \phi \tilde{S}_i^y + \exp(i\mathbf{Q}\mathbf{R}_i) \sin \phi \tilde{S}_i^x, \quad S_i^z = \tilde{S}_i^z. \end{aligned} \quad (\text{A2})$$

Here $\mathbf{Q} = (\pi, \pi)$ and $\exp(i\mathbf{Q}\mathbf{R}_i) = +(-)1$ for i belonging to A (B) sublattice. With this transformation, the anisotropic Hamiltonian Eq. A1, with the above parameterization of coupling constants, is mapped in the rotated frame to the isotropic Heisenberg AF (IHAF)

$$\tilde{\mathcal{H}}_{ij} = J_{ab} \vec{\tilde{S}}_i \cdot \vec{\tilde{S}}_j. \quad (\text{A3})$$

Thus in the rotated frame spins form collinear Néel order. The Hund's coupling induced anisotropy selects in-plane AF order (see Ref. [3]), and corresponding spin pattern in the laboratory frame is given by canted AF structure with canting angle ϕ [see inset in Fig. 4 of the main text].

Based on the above derived mapping, we relate the magnetic susceptibilities of the system described by anisotropic Hamiltonian Eq. A1 to that of isotropic IHAF

Eq. A3. To this end, we first rewrite the transformation Eq. A2 in the momentum representation

$$\begin{aligned} S_{\mathbf{q}}^x &= \cos \phi \tilde{S}_{\mathbf{q}}^x - \sin \phi \tilde{S}_{\mathbf{q}+\mathbf{Q}}^y, \\ S_{\mathbf{q}}^y &= \cos \phi \tilde{S}_{\mathbf{q}}^y + \sin \phi \tilde{S}_{\mathbf{q}+\mathbf{Q}}^x, \quad S_{\mathbf{q}}^z = \tilde{S}_{\mathbf{q}}^z, \end{aligned} \quad (\text{A4})$$

we then express the in-plane and out-of-plane (along the c -axis) components of uniform static magnetic susceptibility of a single plane, χ_{ab} and χ_c respectively, modeled by Eq. A1 in terms of uniform $\chi_0 = \chi(\mathbf{q} = 0)$ and staggered $\chi^\dagger = \chi(\mathbf{q} = \mathbf{Q})$ static susceptibilities of 2D IHAF:

$$\chi_{ab} = \cos^2 \phi \chi_0 + \sin^2 \phi \chi^\dagger, \quad \chi_c = \chi_0. \quad (\text{A5})$$

It is straightforward to generalize Eq. A5 to a 3D system of coupled layers, such as Sr_2IrO_4 of interest here, we find

$$\chi_{ab} = \cos^2 \phi \chi_0 + \sin^2 \phi \chi_+^\dagger, \quad \chi_c = \chi_0, \quad (\text{A6})$$

where χ_+^\dagger now stands for the susceptibility of coupled layers in response to the applied field modulated in such a way that each A sublattice of different layers influence the same field that is opposite to the one influenced by B sublattices. We next relate χ_+^\dagger to χ^\dagger (staggered susceptibility of 2D IHAF) within the random phase approximation (RPA) [see e.g. Ref. [40]] for the weak interlayer couplings. We find

$$\begin{aligned} \chi_+^\dagger &= \frac{\chi^\dagger}{1 - J_c \chi^\dagger}, \\ \chi_{ab} &= \cos^2 \phi \chi_c + \frac{\sin^2 \phi (g_{ab} \mu_B)^2 \chi^\dagger}{1 - J_c \chi^\dagger} \end{aligned} \quad (\text{A7})$$

where J_c is an effective exchange field from neighboring layers, and χ_+^\dagger and χ^\dagger are given in units of inverse energy. Note that biquadratic coupling b does not contribute to a linear susceptibility of paramagnetic state.

-
- [1] B. J. Kim, H. Jin, S. J. Moon, J. -Y. Kim, B. -G. Park, C. S. Leem, J. Yu, T. W. Noh, C. Kim, S. -J. Oh, J. -H. Park, V. Durairaj, G. Cao, and E. Rotenberg, *Phys. Rev. Lett.* **101**, 076402 (2008).
- [2] B. J. Kim, H. Ohsumi, T. Komesu, S. Sakai, T. Morita, H. Takagi, and T. Arima, *Science* **323**, 1329 (2009).
- [3] G. Jackeli and G. Khaliullin, *Phys. Rev. Lett.* **102**, 017205 (2009).
- [4] A. Kitaev, *Annals of Physics* **321**, 2 (2006).
- [5] G. Cao, J. Bolivar, S. McCall, J. E. Crow, and R. P. Guertin, *Phys. Rev. B* **57**, R11039 (1998).
- [6] S. Fujiyama, H. Ohsumi, T. Komesu, J. Matsuno, B. J. Kim, M. Takata, T. Arima, and H. Takagi, *Phys. Rev. Lett.* **108**, 247212 (2012).
- [7] S. Chakravarty, B. I. Halperin, and D. R. Nelson, *Phys. Rev. B* **39**, 2344 (1989).
- [8] J. Kim, D. Casa, M. H. Upton, T. Gog, Y. -J. Kim, J. F. Mitchell, M. van Veenendaal, M. Daghofer, J. van den Brink, G. Khaliullin, and B. J. Kim, *Phys. Rev. Lett.* **108**, 177003 (2012).
- [9] A. Aharony, O. Entin-Wohlman, and A. B. Harris, in *Dynamical Properties of Unconventional Magnetic Systems*, 1998, edited by A. T. Skjeltorp and D. Sherrington (Kluwer Academic Publisher), p. 281.
- [10] B. Keimer, N. Belk, R. J. Birgeneau, A. Cassanho, C. Y. Chen, M. Greven, M. A. Kastner, A. Aharony, Y. Endoh, R. W. Erwin, and G. Shirane, *Phys. Rev. B* **46**, 14034 (1992).
- [11] F. Wang and T. Senthil, *Phys. Rev. Lett.* **106**, 136402 (2011).
- [12] H. Watanabe, T. Shirakawa, and S. Yunoki, *Phys. Rev. Lett.* **110**, 027002 (2013).
- [13] Z. Y. Meng, Y. B. Kim, and H. Y. Kee, *Phys. Rev. Lett.* **113**, 177003 (2014).
- [14] Y. K. Kim, O. Krupin, J. D. Denlinger, A. Bostwick, E. Rotenberg, Q. Zhao, J. F. Mitchell, J. W. Allen, and B. J. Kim, *Science* **345**, 187 (2014).
- [15] Y. K. Kim, N. H. Sung, J. D. Denlinger, and B. J. Kim, *Nature Physics* **12**, 37 (2016).
- [16] Y. J. Yan, M. Q. Ren, H. C. Xu, B. P. Xie, R. Tao, H. Y. Choi, N. Lee, Y. J. Choi, T. Zhang, and D. L. Feng, *Phys. Rev. X* **5**, 041018 (2015).
- [17] Q. Huang, J. L. Soubeyroux, O. Chmaissem, I. Natali Sora, A. Santoro, R. J. Cava, J. J. Krajewski, and W. F. Peck, Jr., *J. Solid State Chem.* **112**, 355-361 (1994).
- [18] T. Thio, T. R. Thurston, N. W. Preyer, P. J. Picone, M. A. Kastner, H. P. Jenssen, D. R. Gabbe, C. Y. Chen, R. J. Birgeneau, and A. Aharony, *Phys. Rev. B* **38**, 905(R) (1988).
- [19] T. Thio and A. Aharony, *Phys. Rev. Lett.* **73**, 894 (1994).
- [20] Although the magnetization is non-linear against magnetic field below T_N , we define χ as M/H throughout this paper.
- [21] C. Dhital, T. Hogan, Z. Yamani, C. de la Cruz, X. Chen, S. Khadka, Z. Ren, and S. D. Wilson, *Phys. Rev. B* **87**, 144405 (2013).
- [22] Only very tiny fraction of ferromagnetic moments (a few percent of M_{ab}) was seen along the c -axis, highly likely due to small misalignment of the sample in the magnetization measurement. We could reasonably subtract the ferromagnetic admixture from M_c by evaluating the in-plane contribution as $M_{ab} H \sin \theta \times \sin \theta$, where θ denotes the misalignment angle estimated to be $\sim 3^\circ$.
- [23] M. F. Ceting, P. Lemmens, V. Gnezdilov, D. Wulferding, D. Menzel, T. Takayama, K. Ohashi, and H. Takagi, *Phys. Rev. B* **85**, 195148 (2012).
- [24] S. -W. Cheong, J. D. Thompson, and Z. Fisk, *Phys. Rev. B* **39**, 4395 (1989).
- [25] By subtracting the contributions of core diamagnetism, the uniform susceptibility χ_0 is estimated to be 4.2×10^{-4} emu/mol. From the relation $\chi_0 = (g\mu_B)^2 / 2zJ_{ab}$ where z is the number of nearest neighbors and $z = 4$ for Sr_2IrO_4 , we obtain J_{ab} as ~ 40 meV, much smaller than the value estimated from the temperature dependence of magnetic correlation length [6]. We presume that this discrepancy is attributed to the contribution of van Vleck

- susceptibility to the experimental χ_c , which is of the order of 10^{-4} emu/mol in iridates [42].
- [26] M. S. Makivic and H. Q. Ding, Phys. Rev. B **43**, 3562 (1991).
- [27] J. K. Kim and M. Troyer, Phys. Rev. Lett. **80**, 2705 (1998).
- [28] For details of fitting, see Supplemental Materials.
- [29] Even though the anisotropy by Hund's coupling is not appreciable at high temperatures, it serves to stabilize the in-plane canted antiferromagnetic structure rather than the collinear Néel ordering with pseudo-spins directed along the c -axis (The two magnetic structures are degenerate without Hund's coupling) **and becomes important close to the transition temperature** [43].
- [30] M. Isobe, H. Okabe, E. Takayama-Muromachi, A. Koda, S. Takeshita, M. Hiraishi, M. Miyazaki, R. Kadono, Y. Miyake, and J. Akimitsu, J. Phys: Conference Series **400**, 032028 (2012).
- [31] S. Boseggia, H. C. Walker, J. Vale, R. Springell, Z. Feng, R. S. Perry, M. Moretti Sala, H. M. Rønnow, S. P. Collins, and D. F. McMorrow, J. Phys.: Condens. Matter **25**, 422202 (2013).
- [32] M. K. Crawford, M. A. Subramanian, R. L. Harlow, J. A. Fernandez-Baca, Z. R. Wang, and D. C. Johnston, Phys. Rev. B **49**, 9198 (1994).
- [33] **When changing to the rotated frame, negligibly small anisotropy terms $\sim \sin \phi J''_{1c}$ have been omitted in Eq. (4.5).**
- [34] We cannot determine the signs of J'_{1c} and J''_{1c} in this model, and the only required constraint is $j_{1c} > 0$ for the ferromagnetic coupling of \vec{m}_n and \vec{m}_{n+1} . For the next-nearest interlayer coupling, J_{2c} must be ferromagnetic (< 0) to realize the antiferromagnetic configuration of \vec{m}_n and \vec{m}_{n+2} [see Fig. 1(a)], and we thus put minus sign in $j_{2c} = -J_{2c}\cos 2\phi$.
- [35] T. Yildirim, A. B. Harris, O. Entin-Wohlman, and A. Aharony, Phys. Rev. Lett. **72**, 3710 (1994).
- [36] T. A. Kaplan, Phys. Rev. B **80**, 012407 (2009)
- [37] In the estimate, we assumed $J_{ab} = 0.13$ eV and Coulomb $U = 5$ eV for La_2CuO_4 and $J_{ab} = 0.10$ eV and $U = 2$ eV for Sr_2IrO_4 . t_\perp is obtained from $J_{\text{out}} = t_\perp^2/U$, and S is taken as 1/2 for both compounds.
- [38] D. Haskel, G. Fabbris, M. Zherenkov, P. P. Kong, C. Q. Jin, G. Cao, and M. van Veenendaal, Phys. Rev. Lett. **109**, 027204 (2012).
- [39] I. Franke, P. J. Baker, S. J. Blundell, T. Lancaster, W. Hayes, F. L. Pratt, and G. Cao, Phys. Rev. B **83**, 094416 (2011).
- [40] D. J. Scalapino, Y. Imry, and P. Pincus, Phys. Rev. B **11**, 2042 (1975).
- [41] K. Momma and F. Izumi, J. Appl. Crystallogr. **44**, 1272 (2011).
- [42] J. Chaloupka, G. Jackeli, and G. Khaliullin, Phys. Rev. Lett. **110**, 097204 (2013).
- [43] **J. G. Vale, S. Boseggia, H. C. Walker, R. Springell, Z. Feng, E. C. Hunter, R. S. Perry, D. Prabhakaran, A. T. Boothroyd, S. P. Collins, H. M. Rønnow, and D. F. McMorrow, Phys. Rev. B **92**, 020406(R) (2015).**